

Towards deep neural network compression via learnable wavelet transforms

Moritz Wolter
University of Bonn
wolter@cs.uni-bonn.de

Shaohui Lin
National University of Singapore
linsh@comp.nus.edu.sg

Angela Yao
National University of Singapore
ayao@comp.nus.edu.sg

April 1, 2022

Abstract

Wavelets are well known for data compression, yet have rarely been applied to the compression of neural networks. In this paper, we show how the fast wavelet transform can be applied to compress linear layers in neural networks. Linear layers still occupy a significant portion of the parameters in recurrent neural networks (RNNs). Through our method, we can learn both the wavelet bases as well as corresponding coefficients to efficiently represent the linear layers of RNNs. Our wavelet compressed RNNs have significantly fewer parameters yet still perform competitively with state-of-the-art on both synthetic and real-world RNN benchmarks. Wavelet optimization adds basis flexibility, without large numbers of extra weights.

1 Introduction

Deep neural networks are routinely used in many artificial intelligence applications of computer vision, natural language processing, speech recognition, etc. However, the success of deep networks has often been accompanied by significant increases in network size and depth. Network compression aims to reduce the computational footprint of deep networks so that they can be applied on embedded, mobile, and low-range hardware. Compression

methods range from quantization [1, 2], pruning [3, 4], to (low-rank) decomposition of network weights [5, 6].

Early methods [5, 3] separated compression from the learning; compression is performed after network training and then followed by fine-tuning. Such a multi-stage procedure is both complicated and may also degrade performance. Ideally, one should integrate compression into the network structure itself; this has the dual benefit of learning less parameters and also ensures that the compression can be accounted for during learning in an end-to-end manner. The more direct form of integrated compression and learning has been adopted in recent approaches [7, 8, 9], typically by enforcing a fixed structure on the weight matrices. Specifically, the structure must lend itself to some form of efficient projection or decomposition in order to have a compression effect, *e.g.* via circulant projections or tensor train decompositions. Maintaining such a structure throughout learning, however, can be challenging, especially using only the first-order gradient descent algorithms favoured in deep learning. Typically, constrained optimization requires managing active and inactive constraints, and or evaluating the Karush-Kuhn-Tucker conditions, all of which can be very expensive. We therefore require alternative ways to enforce weight structure.

One way to simplify the learning is to fix the projection bases *a priori e.g.* to sinusoids, as per the Fourier

transform, or rectangular functions, as per the Walsh-Hadamard transform (WHT) and its derivative the Fast-food transform [10]. The latter has been used to compress the linear layers of CNNs [11, 9]. As it relies on non-local basis functions, the Fastfood transform has a complexity of $O(n \log n)$ for projecting a signal of length n . More importantly, however, using fixed bases limits the network flexibility and generalization power. Since the choice of basis functions determine the level of sparsity when representing data, the flexibility to choose a (more compact) basis could bring significant compression gains.

We advocate the use of wavelets as an alternative for representing the weight matrices of linear layers. Using wavelets offers us two key advantages. Firstly, we can apply the fast wavelet transform (FWT), which has only a complexity of $O(n)$ for projection and comes with a large selection of possible basis functions. Secondly, we can build upon the product filter approach for wavelet design [12] to directly integrate the learning of wavelet bases as a part of training CNNs or RNNs. Learning the bases gives us added flexibility in representing their weight matrices.

Motivated by these advantages, we propose a new linear layer which directly integrates the FWT into its formulation so layer weights can be represented as sparse wavelet coefficients. The compact nature of the wavelet representation can be considered a built in form of network compression. Furthermore, rather than limit ourselves to predefined wavelets as basis functions, we learn the bases directly as a part of network training. Specifically, we adopt the product filter approach to wavelet design. We translate the two hard constraints posed by this approach into soft objectives, which serve as novel wavelet loss terms. By combining these terms with standard learning objectives, we can successfully learn linear layers which using only the wavelet transform, its inverse, diagonal matrices and a permutation matrix. As the reparametrisation is differentiable, it can be trained end-to-end using standard gradient descent.

Our linear layer is general; as we later show in the experiments, it can be applied in both CNNs and RNNs. We focus primarily on gated recurrent units (GRUs), as they typically contain large and dense weight matrices for computing the cell’s state and gate values. Our wavelet-based RNNs are compressed by design and have significantly fewer parameters than standard RNNs, yet still

remain competitive in performance. Through exploring the use of compressed representations on individual cell components, we find a good trade-off between maintaining a large hidden vector state size while reducing the linear layer parameter count. Our main contributions can be summarized as follows:

- We propose a novel method of *learning FWT basis functions* using modern deep learning frameworks by incorporating the constraints of the product filter approach as soft objectives. By learning local basis functions, we are able to reduce the computational cost of the transform to $O(n)$ compared to existing $O(n \log n)$ methods that use fixed non-local basis functions.
- Based on this method, we propose an efficient linear layer which is compressed by design through its wavelet-based representation. This linear layer can be used flexibly in both CNNs and RNNs and allow for large feature or state sizes without the accompanying parameter blowup of dense linear layers.
- Extensive experiments explore the effect of efficient wavelet-based linear layers on the various parts of the GRU cell machinery. Our approach demonstrates comparable or better compression performance compared to state-of-the-art model compression methods.

2 Related Work

2.1 Structured Efficient Linear Transforms

Our proposed approach can be considered a structured efficient linear transform, which replace unstructured dense matrices with efficiently structured ones. There are several types of structures, derived from fast random projections [10], circulant projections [13, 14], tensor train (TT) decompositions [7, 15, 16], low-rank decompositions [17, 5, 18]

One of the main difficulties in using structured representation is maintaining the structure throughout learning. One line of work avoids this by simply doing away with the constraints during the learning phase. For example, low-rank decompositions [17, 5, 18] split the learned

dense weights into two low-rank orthogonal factors. The low-rank constraint then gradually disappears during the fine-tuning phase. The resulting representation is uncontrolled, and must trade off between the efficiency of the low rank and effectively satisfying the fine-tuning objective. In contrast, our proposed soft constraints can be applied jointly with the learning objective, and as such, not only does not require fine-tuning, but can ensure structure throughout the entire learning process.

Within the group of structured efficient linear transforms, the one most similar to the FWT that we are using is the Fastfood transform [11]. The fastfood transform is applied to reparameterize linear layers as a combination of 5 types of matrices: three random diagonal matrices, a random permutation matrix and a Walsh-Hadamard matrix. However, these three diagonal matrices are fixed after random initialization, resulting in a non-adaptive transform. Its fixed nature limits the representation power. As a remedy, [9] proposed an adaptive version in which the three diagonal matrices are optimized through standard backpropagation. Nevertheless, the approach still uses a fixed Walsh-Hadamard basis which may limit the generalization and flexibility of the linear layer. In contrast to the adaptive Fastfood transform, our method is more general and reduces computational complexity.

2.2 Compressing Recurrent Neural Networks

Compressing recurrent cells can be highly challenging; the recurrent connection forces the unit to be shared across all time steps in a sequence so minor changes in the unit can have a dramatic change in the output. To compress RNNs, previous approaches have explored pruning [19, 20], quantization [21] and structured linear transforms [15, 16, 22, 23].

The use of structured efficient linear transforms for compressing RNNs has primarily focused on using tensor decompositions, either via tensor train decomposition [15, 16] or block-term tensor decomposition [23]. The tensor decomposition replaces linear layers with tensors with a lower number of weights and operations than the original matrix. Tensor train decomposition can compress the input-to-hidden matrix in RNNs, but requires the restricted setting on the hyperparameters (*e.g.* ranks

and the restrained order of core tensors) making the compressed models sensitive to parameter selection [15]. Pan *et al.* [22] employ low-rank tensor ring decomposition to alleviate the strict constraints in tensor train decomposition. However, these methods need to approximate the matrix-vector operation by tensor-by-tensor multiplication, where the dense weights and input vectors are reshaped into higher-order tensors. This requires additional reshaping time and generates feature-agnostic representations during training. In contrast, our method shows more flexibility and efficiency performing on the fast wavelet transform, whose bases satisfy with wavelet design using soft objectives.

3 Method

3.1 Fast Wavelet Transform

The wavelet transform projects signals into a multi-resolution spectral domain defined by the wavelet basis of choice. The wavelets themselves are oscillating basis functions derived from scaling and translating a prototypical mother wavelet function such as the Haar, Mexican hat, Daubechies, etc. We refer the curious reader to the excellent primer [12] for a thorough treatment on the topic. For our purposes, we can consider the wavelet transform as being analogous to the Fourier transform. Similarly, wavelets are akin to sinusoids, with a key distinction however, that wavelets are localized basis functions, *i.e.* are not infinite.

Similar to the fast Fourier transform, there exists a fast wavelet transform \mathcal{W} and an inverse \mathcal{W}^{-1} which can be expressed as matrix multiplications [12]:

$$\mathcal{W}(\mathbf{x}) = \mathbf{A}\mathbf{x} = \mathbf{b}, \quad (1)$$

$$\mathcal{W}^{-1}(\mathbf{b}) = \mathbf{S}\mathbf{b} = \mathbf{x}. \quad (2)$$

Given a signal \mathbf{x} indexed by n , the forward wavelet transform yields coefficients b_{jk} in vector \mathbf{b} , which projects \mathbf{x} onto the wavelet basis \mathbf{A} . Matrices \mathbf{A} and \mathbf{S} are referred to as analysis (or forward) and synthesis (or backward) matrices respectively. They are inverses of each other, *i.e.* $\mathbf{A} = \mathbf{S}^{-1}$, and all for reconstruction of the signal from the wavelet coefficients. The double indices jk of b_{jk} denote the scale j and time k positions of each coefficient.

Coefficients b_{jk} can be found by recursively convolving \mathbf{x} with the analysis filters \mathbf{h}_0 and \mathbf{h}_1 with a stride of 2. This process is depicted in Figure 1. The number of scales (6 in our case) is chosen depending on the problem. As a result of the strided convolution, the number of time steps is halved after each scale step. By working backwards through the scales, one can reconstruct $\hat{\mathbf{x}}$ from b_{jk} through transposed convolutions with the synthesis filters \mathbf{f}_0 and \mathbf{f}_1 .

3.2 Learning Wavelet Bases

Typically, wavelets basis functions are selected from a library of established wavelets, *e.g.* as the rectangular functions of Haar wavelet, or arbitrarily designed by hand by the practitioner. Based on the product filter approach, designed wavelets must fulfill conditions of perfect reconstruction and alias cancellation [12]. Given filters \mathbf{h} and \mathbf{f} as well as their z -transformed counterparts $H(z) = \sum_n \mathbf{h}(n)z^{-n}$ and $F(z)$ respectively, the reconstruction condition can be expressed as

$$H_0(z)F_0(z) + H_1(z)F_1(z) = 2z^l, \quad (3)$$

and the anti-aliasing condition as

$$H_0(-z)F_0(z) + H_1(-z)F_1(z) = 0. \quad (4)$$

For the perfect reconstruction condition in Eq. 3, the center term z^l of the resulting z -transformed expression must be a two; all other coefficients should be zero. l denotes the power of the center.

To enforce these constraints in a learnable setting, we can design corresponding differentiable loss terms which we call a wavelet loss. Instead of working in the z -space, we leverage the equivalence of polynomial multiplication and coefficient convolution $(*)$ and reformulate Eq. 3 as:

$$\mathcal{L}_{pr}(\theta_w) = \sum_{k=0}^N \left[(\mathbf{h}_0 * \mathbf{f}_0)_k + (\mathbf{h}_1 * \mathbf{f}_1)_k - \mathbf{0}_{2,k} \right]^2, \quad (5)$$

where $\mathbf{0}_2$ is a zero vector with a two at z^l in its center. This formulation amounts to a measure of the coefficient-wise squared deviation from the perfect reconstruction condition. For alias cancellation, we observe that Eq. 4 is satisfied if $F_0(z) = H_1(-z)$ and $F_1(z) = -H_0(-z)$ and

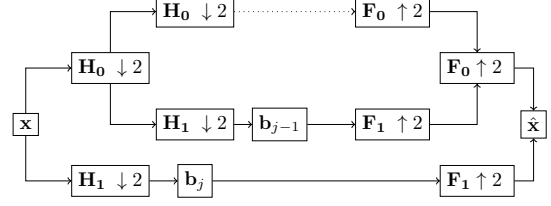


Figure 1: Efficient wavelet signal analysis and synthesis following a tree structure. [12]. \mathbf{H} denotes analysis filters and \mathbf{F} stands for synthesis filters. Up (\uparrow) and down (\downarrow)-sampling by a factor of two is written as the arrow followed by the factor. Filtering and sampling can be accomplished jointly in deep learning frameworks by using strided convolutions for analysis and strided transposed convolutions for synthesis. In place of the dotted arrow more scale-levels can be included.

formulate our anti-aliasing loss as:

$$\mathcal{L}_{ac}(\theta_w) = \sum_{k=0}^N \left(f_{0,k} - (-1)^k h_{1,k} \right)^2 + \left(f_{1,k} + (-1)^k h_{0,k} \right)^2. \quad (6)$$

This formulation leads to the common alternating sign pattern, which we will observe later. We refer to the sum of the two terms in Eqs. 5 and 6 as a wavelet loss. It can be added to standard loss functions in the learning of neural networks.

3.3 Efficient Wavelet-based Linear Layers

To use the efficient wavelet-based linear layer, we begin by decomposing the weight matrices \mathbf{W} as follows:

$$\mathbf{W} = \mathbf{D}\mathcal{W}^{-1}\mathbf{G}\mathbf{\Pi}\mathbf{W}\mathbf{B}, \quad (7)$$

where $\mathbf{D}, \mathbf{G}, \mathbf{B}$ are diagonal learnable matrices of size $n \times n$, and $\mathbf{\Pi} \in \{0, 1\}^{n \times n}$ is a random permutation matrix, which stays fixed during training. We use identity matrices as initialization for $\mathbf{D}, \mathbf{G}, \mathbf{B}$. \mathcal{W} and \mathcal{W}^{-1} denote the wavelet transform and its inverse, which can also be optimized during training. This approach is similar to [9], which relies on the fast Welsh-Hadamard transform. $\mathbf{D}, \mathbf{G}, \mathbf{B}$ and $\mathbf{\Pi}$ can be evaluated in $O(n)$ [24]. The fast wavelet transform requires only $O(n)$ steps instead

of the $O(n \ln n)$ used by the non-local fast Fourier and fast Welsh-Hadamard transforms [12, page 29]. This is asymptotically faster than the transforms used in [9] and [24], who work with fixed Welsh-Hadamard and Fourier transforms. Non square cases where the number of inputs is larger than n can be handled by concatenating square representations with tied wavelet weights, see [9].

We can replace standard weights in linear layers with the decomposition described above, and learn the matrices in Eq. 7 using wavelet loss as defined in Eq. 5 and 6 jointly with the standard network objective. Given the network parameters θ and all filter coefficients θ_w we minimize:

$$\min(\mathcal{L}(\theta)) = \min[(\mathcal{L}_o(\theta)) + \mathcal{L}_{pr}(\theta_w) + \mathcal{L}_{ac}(\theta_w)], \quad (8)$$

where $\mathcal{L}_o(\theta)$ the original loss function (*e.g.* cross-entropy loss) of the uncompressed network, and $\mathcal{L}_{pr}(\theta_w) + \mathcal{L}_{ac}(\theta_w)$ the extra terms for the learnable wavelet basis.

Our wavelet-based linear layer can be applied to fully-connected layers in CNNs and RNNs. For example, suppose we are given a gated recurrent unit (GRU) as follows:

$$\mathbf{g}_r = \sigma(\mathbf{W}_r \mathbf{h}_{t-1} + \mathbf{V}_r \mathbf{x}_t + \mathbf{b}_r), \quad (9)$$

$$\mathbf{g}_z = \sigma(\mathbf{W}_z \mathbf{h}_{t-1} + \mathbf{V}_z \mathbf{x}_t + \mathbf{b}_z), \quad (10)$$

$$\mathbf{z}_t = \mathbf{W}_t(\mathbf{g}_r \odot \mathbf{h}_{t-1}) + \mathbf{V}_t \mathbf{x}_t + \mathbf{b}_t, \quad (11)$$

$$\mathbf{h}_t = \mathbf{g}_z \odot \tanh(\mathbf{z}_t) + (1 - \mathbf{g}_z) \odot \mathbf{h}_{t-1}, \quad (12)$$

where $\sigma(\cdot)$ and $\tanh(\cdot)$ are sigmoid and tanh activation functions, \mathbf{z}_t is the candidate hidden layer values, \mathbf{h}_t is the hidden layer state at the t -th time, and $\mathbf{g}_r, \mathbf{g}_z$ are the reset and update gates, respectively. We can learn efficient gating units by applying the representation from Eq. 7 to the recurrent weight matrices $\mathbf{W}_t, \mathbf{W}_r$ and \mathbf{W}_z . The recurrent weight matrices are of size $n_h \times n_h$ and are typically the largest matrices in a GRU and learning efficient versions of them can reduce the number of network parameters up to 90%.

4 Experiments

We evaluate the effectiveness of our linear layer in both CNNs and RNNs. For CNNs, we select LeNet-5 on MNIST digit recognition classification benchmark [25] as a baseline. For RNNs, we test several GRU models

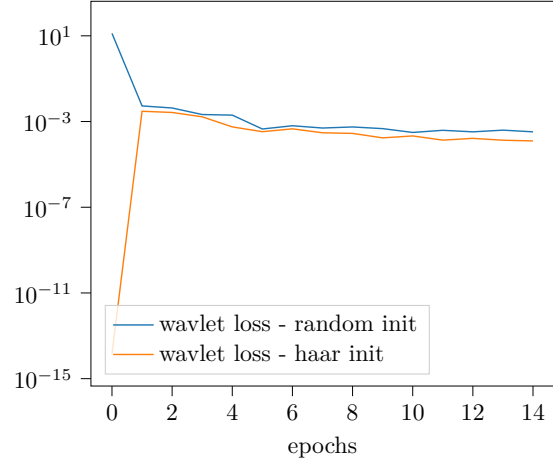


Figure 2: Wavelet loss sum of a randomly and haar initialized wavelet array. In both cases, filter values converge to a product filter as indicated by trend of the wavelet loss towards zero.

on sequence learning tasks including the copy-memory and adding problem [26], sequential MNIST and Penn-Treebank (PTB) character modelling [27].

4.1 MNIST-Digit Recognition

We first apply our efficient wavelet layers to the MNIST digit recognition problem [25]. MNIST has 60K training and 10K test images with a size of 28×28 from 10 classes. We train using an Adadelta optimizer for 14 epochs using a learning rate of 1. The adaptive Fastfood transform is replaced with our proposed learnable-wavelet compression layer. In this feed-forward experiment, we apply dropout to the learned diagonal matrices $\mathbf{D}, \mathbf{G}, \mathbf{B}$ in Eq. 7.

We start by randomly initializing the wavelet array, consisting of 6 parameters per filter, with values drawn from the uniform distribution \mathcal{U}_{-1}^1 . In this case, the initial condition is not a valid product filter so the wavelet loss is initially very large, as shown in Figure 2. However, as this loss term decreases as the random values in the wavelet array start to approximately satisfy the conditions of Eq. 3 and Eq. 4. Correspondingly, the accuracy also rises. With the random initialization we achieve a recognition accuracy of 98.33% with only 36k parameters. We visualize the learned filters in Figure 3. The alias

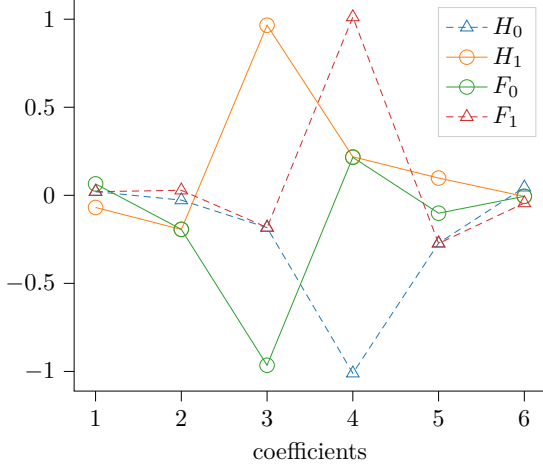


Figure 3: Learned wavelet filter coefficients. Coefficients have been initialized at random. After training, the effects of the alias cancellation constraint are prominently visible. We must have $F_0(z) = H_1(-z)$ and $F_1(z) = -H_0(-z)$ for alias to cancel itself. Inserting $(-z)$ into the coefficient polynomial leads to a minus sign at odd powers. Additional multiplication with (-1) shifts it to even powers. Alias cancellation therefore imposes an alternating sign pattern. When F_0 and H_1 share the same sign F_1 and H_0 do not and vice versa.

Net	Error	Parameters	Reduction
LeNet-5	0.87%	431K	-
LeNet-Fastfood	0.71%	39K	91%
LeNet-random	1.67%	36K	92%
LeNet-Wavelet	0.74%	36K	92%

Table 1: Experimental results on the MNIST digit-recognition. We work with a LeNet architecture as proposed in previous work. In comparison to the fastfood approach [9] we obtain comparable performance with slightly fewer parameters. The size of our learnable-wavelet compression layer is set to 800.

cancellation condition causes an alternating sign pattern. Whenever F_0 and H_1 have the the same sign F_1 and H_0 do not and vice versa. As we observe high recognition rates and small wavelet loss values, we are confident that we have learned valid wavelet basis functions.

Inspired by the Welsh-Hadamard matrix, we also test with a zero-padded Haar wavelet as a initialization; this should ensure a valid FWT at all ties. In this case, the initial wavelet loss is very small as shown in Figure 2, as we already start with a valid wavelet that perfectly satisfies conditions 3 and 4. However, as learning progresses, the condition is no longer satisfied, hence the jump in the loss, before the gradual decrease once again. In Table 1, we compare our result to the Fastfood transform [9]. Our method achieves a comparable result with a higher parameter reduction rate of 92% (vs. 91%), which is quite impressive.

4.2 RNN-Compression

4.2.1 The Copy-Memory and Adding Benchmarks

To explore the effect of our method on recurrent neural networks, we consider the challenging copy-memory and adding tasks as benchmarks [26]. The copy memory benchmark consists out of a sequence of 10 numbers, T zeros, a marker and 10 more zeros. The tested cell observes the input sequence. It must learn to reproduce the original input sequence after the marker. The numbers in the input sequence are drawn from \mathcal{U}_0^n . Element $n + 1$ marks the point where to reproduce the original sequence. We choose to work with $n=8$ in our experiments and use a cross entropy loss. Accuracy is defined as the percentage of correctly memorized integers.

For the adding problem, T random numbers are drawn from \mathcal{U}_0^1 out of which two are marked. The two marks are randomly placed in the first and second half of the sequence. After observing the entire sequence, the network should produce the sum of the two marked elements. A mean squared error loss function is used to measure the difference between the true and the expected sum. We count a sum as correct if $|\hat{y} - y| < 0.05$. We test on GRU cells with a state size of 512. T is set to 150 for the adding problem. Optimization uses a learning rate of 0.001 and RMSprop.

We first explore the effect of our efficient wavelet layer

	Adding problem				Copy-memory problem		
	reduced	mse-loss	accuracy	weights	ce-loss	accuracy	weights
GRU	-	4.9e-4	99.23%	792K	4.8e-5	99.99%	808K
Wave-GRU	\mathbf{z}_t	3.0e-4	99.45%	531K	2.4e-3	99.1%	548K
Wave-GRU	\mathbf{g}_r	1.1e-4	99.96%	531K	3.7e-5	99.98%	548K
Wave-GRU	\mathbf{g}_z	4.4e-4	97.78%	531K	1.1e-1	21.63%	548K
Wave-GRU	$\mathbf{g}_r, \mathbf{g}_z$	0.9e-4	99.85%	270K	3.7e-2	73.63%	288K
Wave-GRU	$\mathbf{z}_t, \mathbf{g}_r$	3.0e-4	98.56%	270K	2.4e-3	99.05%	288K
Wave-GRU	$\mathbf{z}_t, \mathbf{g}_z$	1.1e-3	92.64%	270K	1.2e-1	12.67%	288K
Wave-GRU	$\mathbf{z}_t, \mathbf{g}_r, \mathbf{g}_z$	1.0e-3	91.64%	10K	1.2e-1	16.84%	27K
Ff-GRU	$\mathbf{z}_t, \mathbf{g}_r, \mathbf{g}_z$	1.3e-3	85.99%	10K	1.2e-1	16.44%	27K

Table 2: RNN compression results on the adding and memory problems, exploring the impact of our efficient wavelet-based linear layer at various locations in the GRU. On the adding problem all tested variants are functional. Compressing the state and reset equations has virtually no effect on performance. Compressing the update gate leads to a working cell, but cells with a compressed update gate perform significantly worse. Note that on the adding problem, predicting a sum of 1 regardless of the input leads to an mse of 0.167. On the copy-memory benchmark, replacing the the state and reset weight matrices with our efficient wavelet version is possible without significant performance losses. A state size of 512 was used for all models. The expected cross entropy for a random guess is 0.12 with $n=8$.

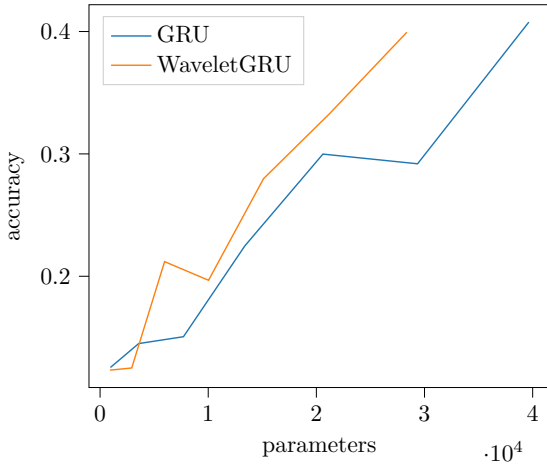


Figure 4: Accuracy and parameters of gated recurrent units with and without a compressed reset gate on the memory problem with $T = 60$. Both models start with 1K parameters. As we increase the state size from 12 to 108, the parameter count rises to 39K for the standard GRU and to 29K for the compressed version. We observe that reset gate compression increases parameter efficiency in this case.

on the reset g_r and update g_z equations (Eq. 9, 10) as well as the state z_t equation (Eq. 11). As shown in Table 2, We observed that efficient representations of the state and reset equations has little impact on performance, while significantly reducing the weights. In the combined case, our method has $2.8\times$ less parameters than dense weight matrices with only 0.91% accuracy drop in copy memory problem. For the adding problem, our method achieves a factor of $2.9\times$ reduction with only 0.67% accuracy drop. When incorporating this into multiple weight matrices, we find that using the efficient representation is problematic for the update matrix W_z next state computation. We found that compressing the update gate has a large impact on the performance, especially the combination with state compression. The update mechanism plays an important role for stability and should not be compressed.

Compared to the Fastfood transform [9], our method is better at compressing entire cells. It achieves higher accuracy with the same number of weights both in adding problem and copy memory problem. For example, in adding problem, our method achieves a higher accuracy of 91.64% (vs. 85.99%) with the same number of weights, compared to the Fastfood transform [9]. Figure 4 compares the relationship of weight growth and accuracy for

Sequential MNIST					Penn Treebank Character Prediction				
	reduced	loss	acc.	weights		reduced	loss	bpc	weights
GRU	-	6.49e-2	100%	795K	TCN	-	0.916	1.322	2,221K
Wave-GRU	$\mathbf{z_t}$	8.98e-2	98%	534K	GRU	-	0.925	1.335	972K
Wave-GRU	$\mathbf{g_r}$	6.06e-2	100%	534K	Wave-GRU	$\mathbf{z_t}$	0.97	1.399	711K
Wave-GRU	$\mathbf{g_z}$	1.82	26%	534K	Wave-GRU	$\mathbf{g_r}$	0.925	1.335	711K
Wave-GRU	$\mathbf{g_r, g_z}$	1.33	46%	274K	Wave-GRU	$\mathbf{z_t, g_r}$	0.969	1.398	450K
Wave-GRU	$\mathbf{z_t, g_r}$	9.48e-2	98%	274K					
Wave-GRU	$\mathbf{z_t, g_z}$	1.60	34%	274K					
Wave-GRU	$\mathbf{z_t, g_z, g_r}$	1.52	36%	13K					
WaveGRU-64	$\mathbf{z_t, g_r}$	0.127	96.4%	4.9K					
TT-GRU	-	-	98.3%	5.1K					

Table 3: RNN compression results on the sequential MNIST benchmark. The pattern here reflects what we saw on the adding and copy-memory benchmarks. Touching the update gate has a negative impact. All other equations can be compressed. our method (WaveGRU-64) achieves a comparable performance, compared to [15].

reset compression and a standard GRU on the memory problem. We observe that the compressed case is more efficient.

4.2.2 Sequential-MNIST

The sequential MNIST benchmark dataset has previously been described in Section 4.1. A gray-scale image with a size of 28×28 is interpreted as a sequence of 784 pixels. The entire sequence is an input to the GRU, which will generate a classification score. We select a GRU with a hidden size of 512 as our baseline and an RMSProp optimizer with a learning rate of 0.001.

Results of our method are shown in Table 3. Similar to the results of Table 2, we also observe that having efficient representations for the state and reset gate matrices work well, but compressing the update gate adversely impacts the results. Compared to only state compression, the combination of state and reset compression achieves a higher compression rate of $2.9 \times$ (vs. $1.5 \times$), without the accuracy drop. We also compare to the tensor train approach used in [15]. We apply the efficient wavelet layer only on the reset and state weight matrices and reduce the cell size to 64. Our approach does reasonably well with

fewer parameters.

4.2.3 Penn Treebank Character Modelling

We verify our approach on the Penn-Treebank (PTB) character modelling benchmark [27]. We split the dataset into training, validation and test sequences, which contains 5,059K training characters, 396K validation characters and 446K testing characters. Given an input sequence of 320 characters, the model should predict the next character. We work with a GRU of size 512 trained using an Adam optimizer with an initial learning rate of 0.005. Training is done using a cross entropy loss in addition to the wavelet loss, and results are reported using bits per character (bpc), where lower bpc is better. In Table 4, we show results for a temporal convolutional network (TCN) [28], a vanilla GRU cell as well as state, reset and state reset compression, which we found to be successfully earlier. We confirm that our wavelet-based compression method can be used to compress reset gate and cell state without significant performance loss.

5 Conclusion

We presented a novel wavelet based efficient linear layer which demonstrates competitive performance within convolutional and recurrent network structures. On the MNIST digit recognition benchmark, we show state of the art compression results as well as convergence from randomly initialized filters.

We explore RNN compression and observe comparable performance on the sequential MNIST task. In a gated recurrent unit we can compress the reset and state equations without a significant impact on performance. The update gate equation was hard to compress, in particular in combination with the state equation. Joint update gate and reset gate equation compression generally worked better than update and state compression. We conclude that the update mechanism plays the most important role within a GRU-cell, followed by the state equation and finally the reset gate. Results indicate that selective compression can significantly reduce cell parameters while retaining good performance.

Product filters are only one way of wavelet design, alternative methods include lifting or spectral factorization approaches. We look forward to exploring some of these in the future. Efficient implementation of the FWT on GPUs is no simple matter. We will open our framework upon acceptance of this paper in the hope that it will spark future work on highly optimized implementations.

References

- [1] Matthieu Courbariaux, Yoshua Bengio, and Jean-Pierre David. Binaryconnect: Training deep neural networks with binary weights during propagations. In *NIPS*, 2015.
- [2] Mohammad Rastegari, Vicente Ordonez, Joseph Redmon, and Ali Farhadi. Xnor-net: Imagenet classification using binary convolutional neural networks. In *ECCV*, pages 525–542. Springer, 2016.
- [3] Song Han, Jeff Pool, John Tran, and William Dally. Learning both weights and connections for efficient neural networks. In *NIPS*, pages 1135–1143, 2015.
- [4] Shaohui Lin, Rongrong Ji, Yuchao Li, Yongjian Wu, Feiyue Huang, and Baochang Zhang. Accelerating convolutional networks via global & dynamic filter pruning. In *IJCAI*, pages 2425–2432, 2018.
- [5] Emily L Denton, Wojciech Zaremba, Joan Bruna, Yann LeCun, and Rob Fergus. Exploiting linear structure within convolutional networks for efficient evaluation. In *NIPS*, pages 1269–1277, 2014.
- [6] Shaohui Lin, Rongrong Ji, Xiaowei Guo, and Xue-long Li. Towards convolutional neural networks compression via global error reconstruction. In *IJCAI*, 2016.
- [7] Alexander Novikov, Dmitrii Podoprikin, Anton Osokin, and Dmitry P Vetrov. Tensorizing neural networks. In *NIPS*, pages 442–450, 2015.
- [8] Yani Ioannou, Duncan Robertson, Roberto Cipolla, and Antonio Criminisi. Deep roots: Improving cnn efficiency with hierarchical filter groups. In *CVPR*, 2017.
- [9] Zichao Yang, Marcin Moczulski, Misha Denil, Nando de Freitas, Alex Smola, Le Song, and Ziyu Wang. Deep fried convnets. In *ICCV*, pages 1476–1483, 2015.
- [10] Nir Ailon and Bernard Chazelle. The fast johnson–lindenstrauss transform and approximate nearest neighbors. *SIAM Journal on computing*, 39(1):302–322, 2009.
- [11] Quoc Le, Tamás Sarlós, and Alex Smola. Fastfood: approximating kernel expansions in loglinear time. In *ICML*, volume 85, 2013.
- [12] Gilbert Strang and Truong Nguyen. *Wavelets and filter banks*. SIAM, 1996.
- [13] Yu Cheng, Felix X Yu, Rogerio S Feris, Sanjiv Kumar, Alok Choudhary, and Shi-Fu Chang. An exploration of parameter redundancy in deep networks with circulant projections. In *ICCV*, pages 2857–2865, 2015.
- [14] Alexandre Araujo, Benjamin Negrevergne, Yann Chevalere, and Jamal Atif. Training compact deep learning models for video classification using circulant matrices. In *ECCV*, pages 0–0, 2018.
- [15] Andros Tjandra, Sakriani Sakti, and Satoshi Nakamura. Compressing recurrent neural network with tensor train. In *IJCNN*, pages 4451–4458. IEEE, 2017.
- [16] Yinchong Yang, Denis Krompass, and Volker Tresp. Tensor-train recurrent neural networks for video

- classification. In *ICML*, pages 3891–3900. JMLR. org, 2017.
- [17] Misha Denil, Babak Shakibi, Laurent Dinh, Marc’Aurelio Ranzato, and Nando De Freitas. Predicting parameters in deep learning. In *NIPS*, pages 2148–2156, 2013.
 - [18] Max Jaderberg, Andrea Vedaldi, and Andrew Zisserman. Speeding up convolutional neural networks with low rank expansions. *arXiv preprint arXiv:1405.3866*, 2014.
 - [19] Wei Wen, Yuxiong He, Samyam Rajbhandari, Minjia Zhang, Wenhan Wang, Fang Liu, Bin Hu, Yiran Chen, and Hai Li. Learning intrinsic sparse structures within long short-term memory. *arXiv preprint arXiv:1709.05027*, 2017.
 - [20] Sharan Narang, Erich Elsen, Gregory Diamos, and Shubho Sengupta. Exploring sparsity in recurrent neural networks. *arXiv preprint arXiv:1704.05119*, 2017.
 - [21] Zhisheng Wang, Jun Lin, and Zhongfeng Wang. Accelerating recurrent neural networks: A memory-efficient approach. *IEEE Transactions on Very Large Scale Integration (VLSI) Systems*, 25(10):2763–2775, 2017.
 - [22] Yu Pan, Jing Xu, Maolin Wang, Jinmian Ye, Fei Wang, Kun Bai, and Zenglin Xu. Compressing recurrent neural networks with tensor ring for action recognition. In *AAAI*, volume 33, pages 4683–4690, 2019.
 - [23] Jinmian Ye, Linnan Wang, Guangxi Li, Di Chen, Shandian Zhe, Xinqi Chu, and Zenglin Xu. Learning compact recurrent neural networks with block-term tensor decomposition. In *CVPR*, pages 9378–9387, 2018.
 - [24] Martin Arjovsky, Amar Shah, and Yoshua Bengio. Unitary evolution recurrent neural networks. In *ICML*, pages 1120–1128, 2016.
 - [25] Yann LeCun, Léon Bottou, Yoshua Bengio, Patrick Haffner, et al. Gradient-based learning applied to document recognition. *Proceedings of the IEEE*, 86(11):2278–2324, 1998.
 - [26] Sepp Hochreiter and Jürgen Schmidhuber. Long short-term memory. *Neural computation*, 9(8):1735–1780, 1997.
 - [27] Mitchell Marcus, Beatrice Santorini, and Mary Ann Marcinkiewicz. Building a large annotated corpus of english: The penn treebank. 1993.
 - [28] Shaojie Bai, J. Zico Kolter, and Vladlen Koltun. An empirical evaluation of generic convolutional and recurrent networks for sequence modeling. *arXiv:1803.01271*, 2018.